Employment of Gibbs-Donnan-based concepts for interpretation of the properties of linear polyelectrolyte solutions

ARTICLE *in* THE JOURNAL OF PHYSICAL CHEMISTRY · NOVEMBER 1991

Impact Factor: 2.78 · DOI: 10.1021/j100177a106

Reprinted from The Journal of Physical Chemistry, 1991, 95.

Employment of Gibbs–Donnan-Based Concepts for Interpretation of the Properties of Linear Polyelectrolyte Solutions

Jacob A. Marinsky* and Michael M. Reddy†

Department of Chemistry, State University of New York at Buffalo, Buffalo, New York 14214
(Received: December 17, 1990; In Final Form: July 15, 1991)

Earlier research has shown that the acid dissociation and metal ion complexation equilibria of linear, weak-acid polyelectrolytes and their cross-linked gel analogues are similarly sensitive to the counterion concentration levels of their solutions. Gibbs–Donnan-based concepts, applicable to the gel, are equally applicable to the linear polyelectrolyte for the accommodation of this sensitivity to ionic strength. This result is presumed to indicate that the linear polyelectrolyte in solution develops counterion-concentrating regions that closely resemble the gel phase of their analogues. Advantage has been taken of this description of linear polyelectrolytes to estimate the solvent uptake by these regions.

I. Introduction

In our examination of the acid dissociation[1-3] and metal ion complexation[4,5] properties of cross-linked, weak-acid polyelectrolyte gels and the ion-exchange behavior of the Linde A zeolite[6] Gibbs–Donnan-based concepts[7-9] were shown to provide quantitative interpretations of the results obtained. Application of these same concepts to the analysis of the acid dissociation[10] and metal ion complexation equilibria[11] of the linear, weak-acid polyelectrolyte analogues of the cross-linked gels was equally successful. This result is believed to show that the linear polyelectrolyte in solution develops counterion-concentrating regions that closely resemble the gel phase of the cross-linked analogue.[10] It is pictured as the charge center of a solvent sheath from which only a small fraction of counterions escapes to the solution.

This description of linear polyelectrolytes in solution, first proposed by one of us (J.A.M.) in 1973,[12] is compatible with the physical picture one derives from Manning's mathematically dictated counterion condensation model first introduced in 1969.[13] According to Manning's model counterions are transferred into the region next to the surface of the oppositely charged polyion (our solvent sheath) when the distance, b, between charged sites of the polyion is equal to or less than a Bjerrum length of $7.14Z$ Å, where Z is the charge of the counterion. The territorially bound counterions are presumed to move freely along the surface of the polyion but not away from it.[13-15] Equation 1 was derived for

$$V_p = 41.1(\xi - 1)b^3 \qquad (1)$$

estimating the volume, V_p, of the zone of counterion condensation that was presumed to prevail as long as ξ, the charge density parameter, defined as $7.14Z/b$ Å, exceeded a value of unity.[14] Whereas there is always a solvent sheath to be encountered in our conception of polyelectrolytes in solution, this is not the case with the counterion condensation model.[16] In addition, V_p is uniquely defined by the structurally based b value, while variability of this parameter is an essential aspect of our approach.

It is the objective of this particular study to examine this operational picture of the linear polyelectrolyte in solution in greater depth. It was expected that application of Gibbs–Donnan-based concepts to the two separate regions presumed to control the equilibrium properties of polyelectrolytes in solution would facilitate a meaningful description of them. In particular, it was expected that such an examination would lead to resolution of the water content of the solvent sheath presumed to constitute the counterion-concentrating domain considered to be associated with the charged surface of the polyelectrolyte.

Data compiled in earlier research by us to measure the effect of substituting the linear, strong-acid, poly(styrenesulfonic acid) for perchloric acid on the ion-exchange distribution of H^+ ion and trace-level concentrations of divalent metal ion between Dowex 50, the divinylbenzene-cross-linked poly(styrenesulfonic acid) ion-exchange resin, and these two solutions,[17] are ideally suited for this purpose. They have consequently been used in this study to facilitate these objectives.

II. Basis of Research

(A) Operational Picture. A solvated region, presumed to border the fully dissociated, linear polyelectrolyte molecule, is believed to contain most of the counterions needed to neutralize its charge. Such confinement to this region of most of the counterions, which remain free and laterally mobile, is attributed to the electric field projected by the charged polyelectrolyte surface. Only those counterions that escape the solvated zone are accessible to measurement; they define the colligative properties of the solution.

Experimental confirmation of this operational picture is provided by the additivity of the colligative properties of polyelectrolyte and simple salt solutions when they are in solution together.[18-20]

(B) Gibbs–Donnan-Based Description of the Distribution of Counterions in Fully Ionized, Linear Polyelectrolyte Solutions. Gibbs–Donnan-based concepts can be employed to examine further the credibility of the above operational picture. If, as presumed, the linear, fully ionized polyelectrolyte in solution is indeed partitioned as described, one can equate the electrochemical potential, E, of its counterion, C^+, in the two regions at equilibrium:

$$E_c = \bar{E}_c \qquad (2)$$

†U.S. Geological Survey, Water Resources Division, Denver Federal Center, Denver, CO 80225.

(1) Merle, Y.; Marinsky, J. A. *Talanta* **1984**, *31*, 199.
(2) Alegret, S.; Marinsky, J. A.; Escalas, M. T. *Talanta* **1984**, *31*, 683.
(3) Marinsky, J. A.; Miyajima, T.; Högfeldt, E.; Muhammed, M. *Reactive Polym.* **1989**, *11*, 279.
(4) Anspach, W. M.; Marinsky, J. A. *J. Phys. Chem.* **1975**, *79*, 433.
(5) Marinsky, J. A. *J. Chromatogr.* **1980**, *201*, 5.
(6) Bukata, S.; Marinsky, J. A. *J. Phys. Chem.* **1964**, *68*, 994.
(7) Gregor, H. P. *J. Am. Chem. Soc.* **1951**, *73*, 642.
(8) Glueckauf, E. *Proc. R. Soc. London* **1952**, *A214*, 207.
(9) Helfferich, F. *Ion Exchange*; McGraw-Hill: New York, 1962; Chapter 5.
(10) Marinsky, J. A.; Miyajima, T.; Högfeldt, E.; Muhammed, M. *Reactive Polym.* **1989**, *11*, 291.
(11) Travers, C.; Marinsky, J. A. *J. Polym. Sci.* **1974**, *Symp. 47*, 285.
(12) Marinsky, J. A.; Imai, N.; Lim, M. C. *Isr. J. Chem.* **1973**, *11*, 601.
(13) Manning, G. S. *J. Chem. Phys.* **1969**, *51*, 924.
(14) Manning, G. S. *Q. Rev. Biophys.* **1978**, *2*, 179.
(15) Friedman, R. A. G.; Manning, G. S. *Biopolymers* **1984**, *23*, 2671.
(16) Manning, G. S. *J. Phys. Chem.* **1981**, *85*, 870.
(17) Reddy, M. M.; Marinsky, J. A. *J. Macromol. Sci., Phys.* **1971**, *B5*, 135.
(18) Alexandrowicz, Z. *J. Polym. Sci.* **1960**, *43*, 325.
(19) Alexandrowicz, Z. *J. Polym. Sci.* **1960**, *43*, 337.
(20) Katchalsky, A.; Alexandrowicz, T.; Kedem, O. In *Chemical Physics of Ionic Solutions*; Conway, B. E., Barradas, R. G., Eds.; Wiley: New York, 1966; Chapter 15.

0022-3654/91/2095-10208$02.50/0

where the arrow is used to identify the counterion-concentrating domain of the polyelectrolyte. The electrochemical potential of counterion C differs from its chemical potential, μ_c, in each region by a quantity that depends on the electric potential, σ, that the counterion is exposed to, and

$$E_c = \mu_c + Z_c F\sigma = \bar{\mu}_c + Z_c F\bar{\sigma} \tag{3}$$

In eq 3, Z_c represents the valence of the counterion and F is the Faraday constant. The chemical potential of counterion C in each region is defined as

$$\begin{aligned} \mu_c &= \mu_c^\circ + RT \ln a_c + PV_c \\ \bar{\mu}_c &= \bar{\mu}_c^\circ + RT \ln \bar{a}_c + \bar{P}V_c \end{aligned} \tag{4}$$

Here μ_c° is the chemical potential of counterion C in its standard state; a_c corresponds to its activity, V_c to its partial molar volume at infinite dilution, and P to the pressure on the region considered to be involved. By substituting the definitions of E and μ_c given by eqs 3 and 4 in eq 2, we obtain

$$\bar{\sigma} - \sigma = \frac{1}{Z_c F}(RT \ln (a_c/\bar{a}_c) - \pi V_c) \tag{5}$$

μ_c° and $\bar{\mu}_c^\circ$ cancelling with assignment of the same standard state to both regions and π being substituted for $(\bar{P} - P)$. Representation of the equilibrium distribution of a pair of cations, such as H^+ and M^+, with eq 5 then reduces to

$$\ln \frac{(a_{H^+})}{(\bar{a}_{H^+})} \frac{(\bar{a}_{M^+})}{(a_{M^+})} = \frac{\pi[V_H - V_M]}{RT} \simeq 0 \tag{6}$$

$\bar{\sigma} - \sigma$ being cancelled by $\sigma - \bar{\sigma}$.

For the sake of simplicity it has been assumed that the partial molar volumes are independent of composition and pressure. For the solvent this assumption holds fairly well over a wide range of experimental conditions.[9] For the exchanging ions it is the difference in the partial molar volumes of the ions that is important, and exposure of both ions to the same experimental conditions is believed to justify use of partial molar volumes at infinite dilution. Experimental evidence fully supporting this approximation is contained in the zeolite studies of Bukata and Marinsky.[6] In any case, use of this approximation has been avoided to eliminate it as a source of concern.

III. Analysis of the Solution Properties of the Fully Ionized, Linear Polyelectrolyte Poly(styrenesulfonic acid) (HPSS)

To facilitate the objectives of this project, data compiled in an earlier study comparing the distribution of H^+ ion and trace-level concentrations of M^{+2} ion between (1) an ion-exchange resin and $HClO_4$ solutions of varying molality and (2) the same ion-exchange resin and HPSS solutions of varying molality[17,21] were subjected to analysis. Because the physical-chemical properties of the perchloric acid and its trace constituent, $M(ClO_4)_2$, are reasonably well understood, meaningful resin parameters were resolvable with the first set of data. These resin parameters were then usefully employable for assessment of the less easily accessible physical-chemical properties of the polyelectrolyte that are reflected by the different distribution of H^+ ion and M^{+2} ion in the two systems examined in exactly the same manner.

The first set of distribution experiments led to resolution of the product of the resin parameters, $\ln (\bar{\gamma}_{H^+})^2/(\bar{\gamma}_{M^{2+}})$ and $\pi(V_M - 2V_H)/RT$. This quantity, considered to be uniquely applicable to the resin phase in both systems, was used to anticipate the disposition of H^+ and M^{2+} in the two separate zones presumed to characterize solutions of linear, fully ionized polyelectrolytes. Changes in the magnitude of the $\pi(V_M - 2V_H)/RT$ term that are introduced by differences between the water activity of the separate $HClO_4$ and HPSS solutions examined are well within the precision range of the ion-exchange measurements themselves to ensure the reliability of this resin calibration procedure. The resin calibration measurements, by anticipating the distribution of the M^{2+} ion between the resin and the polyelectrolyte region bordering the counterion-concentrating solvent sheath next to the charged surface of the polyelectrolyte, facilitated estimate of the water content of the inner region as well.

(1) Calibration of the Divinylbenzene-Cross-Linked Analogue of the Linear, Fully Ionized HPSS. The quantity, $\ln (\bar{\gamma}_{H^+})^2/(\bar{\gamma}_{M^{2+}}) + \pi(2V_H - V_M)/RT$, essentially undisturbed by the employment of different $HClO_4$ concentration levels in the first set of distribution measurements because of the constancy of the H^+ ion environment of the gel, was determinable with eq 6, modified by substituting molality and activity coefficient products for activities and through the rearrangement of these terms:

$$\ln \frac{(\bar{\gamma}_{H^+})^2}{(\bar{\gamma}_{M^{2+}})} + \frac{\pi}{RT}(2V_H - V_M) = \ln \frac{(\bar{m}_{M^{2+}})}{(\bar{m}_{H^+})^2} \frac{(m_{H^+})^2}{(m_{M^{2+}})} \frac{(\gamma^{\pm}_{HClO_4})^4}{(\gamma^{\pm}_{M(ClO_4)_2})^3} \tag{6a}$$

Here the bar above a symbol is used to identify association with the gel phase. The squaring of the H^+-ion associated terms in eq 6a is necessary, of course, to account for the stoichiometry of the exchange reaction under scrutiny. Use of the literature values of the mean molal activity coefficients of $HClO_4$ and $M(ClO_4)_2$ at the solution ionic strength,[22] as shown, eliminates the contribution of $\gamma_{ClO_4^-}$ so that $(\gamma_{H^+})^2/(\gamma_{M^{2+}})$, the ratio being sought for estimate of $(a_{H^+})^2/(a_{M^{2+}})$, is resolved.

The distribution measurements, at equilibrium, of H^+ ion and trace quantities of M^{2+} in the reference ion-exchange resin, perchloric acid systems that were made available to the calibration program are expressed by the parameter ${}^{M^{2+}}_{H^+}K_{Ex}$:[17,21]

$${}^{M^{2+}}_{H^+}K_{Ex} = \frac{(\bar{m}_{M^{2+}})}{(\bar{m}_{H^+})^2} \frac{(m_{H^+})^2}{(m_{M^{2+}})} \tag{7}$$

$$\ln \frac{(\bar{\gamma}_{H^+})^2}{(\bar{\gamma}_{M^{2+}})} + \frac{\pi}{RT}(2V_H - V_M) = \ln {}^{M^{2+}}_{H^+}K_{Ex} + \ln \frac{(\gamma^{\pm}_{HClO_4})^4}{(\gamma^{\pm}_{M(ClO_4)_2})^3} \tag{6a}$$

Neglect of the effect of ion interaction on the mean molal activity coefficient of $M(ClO_4)_2$, the trace component in these computations, is believed justified. The perturbations one can expect at the low $HClO_4$ concentrations employed for the calibration are small. {From a list of Harned rule coefficients that has been compiled to correct for the effect of NX presence at macrolevel concentrations ranging from 0.5 to 2.0 m on the activity coefficient of MX_2, a trace component ($\log \gamma_{MX_2}(m_{NX}) = \log \gamma_{MX(0)} - \alpha_{MX_2} m_{NX}$), we see that the value of α_{MX_2} does not exceed 0.064. If we presume that in the $HClO_4$, trace $Co(ClO_4)_2$ mixtures employed by us ($0.0406 \geqslant m_{HClO_4} \leqslant 0.168$) that $\alpha_{Co(ClO_4)_2}$ is as large as 0.064, then the maximum error in $(\gamma^{\pm}_{HClO_4})^4/(\gamma^{\pm}_{Co(ClO_4)_2})^3$ of [antilog $3(\alpha_{MX_2} m_{NX}) - 1$][100] that is introduced by neglect of such a correction can vary from a value of 1.8% at $m_{HClO_4} = 0.0406$ to 7.1% at $m_{HClO_4} = 0.168$.}

Harned Rule Coefficients[23]

NX	MX_2 (trace)	α_{NX_2} 0.50 M	1.0 M	2.0 M
NaCl	$MgCl_2$	−0.0061	−0.012	−0.015
NaCl	$CaCl_2$	−0.011	0.0002	−0.013
KCl	$MgCl_2$	−0.064	−0.0475	+0.037
KCl	$CaCl_2$	0.053	0.026	0.0202

(2) Use of the Resin Calibrations for Estimate of the Concentration of Trace Level Quantities of M^{2+} in That Region of Polyelectrolyte Solutions That Is Separate from the Solvent Sheath Circumscribing the Charged Surface of the Polyion. The ion-exchange data collected at several different perchloric acid concentrations in the calibration procedure described earlier are used

(21) Reddy, M. M. Doctoral Thesis, State University of New York at Buffalo, Buffalo, NY, 1970.

(22) Robinson, R. A.; Stokes, R. H. *Electrolyte Solutions*; Butterworths: London, 1959; Appendix 8, 9 and 10, pp 480–501.

TABLE I: Results of a Characterization Study of the H^+ Ion Form of an 8% Divinylbenzene Cross-Linked Poly(styrenesulfonate) Resin (Dowex 50)

$\bar{m}_H$	m_{HClO_4}	K_d	$(\gamma^{\pm}_{HClO_4})^4/(\gamma^{\pm}_{Co(ClO_4)_2})^3$	$\log (a_{H^+})^2/\gamma_{Co^{2+}}$	$\log (\bar{\gamma}_{H^+})^2/(\bar{\gamma}_{Co^{2+}}) + \pi(2V_H - V_{Co})/2.3RT$
4.52	0.0406	23700	1.484	−2.591	0.528
4.52	0.0413	22800	1.476	−2.600	0.473
4.54	0.0672	7548	1.573	−2.149	0.467
4.54	0.0630	9271	1.554	−2.210	0.439
4.58	0.1114	2859	1.744	−1.665	0.412
4.58	0.1086	3016	1.757	−1.684	0.446
4.62	0.168	1342	1.893	−1.272	0.450
					av = 0.461
					σ = 0.0345
					PE = 0.0233

to provide the avenue to $m_{M^{2+}}$ estimates in the polyelectrolyte solutions examined. By rearranging eq 6a, as shown in eq 6b,

$$\ln \frac{\bar{m}_{M^{2+}}}{m_{M^{2+}}} = \ln \frac{(\bar{m}_{H^+})^2}{(m_{H^+})^2} \frac{(\bar{\gamma}_{H^+})^2}{(\gamma_{H^+})^2} \frac{(\gamma_{M^{2+}})}{(\bar{\gamma}_{M^{2+}})} - \frac{\pi(V_M - 2V_H)}{RT} \quad (6b)$$

it becomes apparent that the $\ln \bar{m}_{M^{2+}}/m_{M^{2+}}$ parameter should be directly proportional to $\ln \gamma_{M^{2+}}/(m_{H^+})^2(\gamma_{H^+})^2$, the resin phase parameters $\bar{m}_{H^+}$, $\bar{\gamma}_{H^+}$, $\bar{\gamma}_{M^{2+}}$, and $\pi(V_M - 2V_H)/RT$ remaining essentially unchanged in this series of experiments. The straight line plot of $\log \bar{m}_{M^{2+}}/m_{M^{2+}}$ versus $\log \gamma_{M^{2+}}/(m_{H^+})^2(\gamma_{H^+})^2$ one obtains from these calibration studies has been used to interpolate $\bar{m}_{M^{2+}}/m_{M^{2+}}$ values to be expected when HPSS solutions containing trace level concentrations of M^{2+} are equilibrated with the previously calibrated resin. The values of γ_{H^+} and $\gamma_{M^{2+}}$ employed to facilitate this direction of the research were assigned at the experimental ionic strength by using the single ion activity coefficient compilations of Kielland.[24] For the polyelectrolyte, ionic strength was equated to the value of m_{H^+} obtained by using eq 8. In this equation ϕ_{HPSS} corresponds to the osmotic coefficient

$$m_{H^+} = m_{HPSS}(\phi_{HPSS}) \quad (8)$$

of the HPSS at m_{HPSS}, the molality (monomer basis) of the HPSS. The osmotic coefficient values used in eq 8 were extrapolated from a plot of ϕ_{HPSS} versus m_{HPSS} data available to us from vapor pressure osmometry studies carried out previously.[21,25]

(3) Water Content of the Hypothetical Solvated Region Surrounding the Charged Surface of Linear, Fully Ionized Polyelectrolyte Solutions. With $\bar{m}_{M^{2+}}/m_{M^{2+}}$ made available by the graphical approach, the gross distribution studies carried out with the calibrated resin, polyelectrolyte system now become employable for estimate of $\bar{m}_{M^{2+}}/m_{M^{2+}}$. The quantity measured directly corresponds to the entity $\bar{m}_{M^{2+}}/(m_{M^{2+}} + \sum \bar{q}_{M^{2+}})$, where $\sum \bar{q}_{M^{2+}}$ is the quantity of unaccessible M^{2+} contained by the counter-ion-concentrating domain that is associated with 1 g of the water component of the polyelectrolyte solution. Dividing the numerator and denominator of this quantity by $m_{M^{2+}}$ gives

$$\frac{\bar{m}_{M^{2+}}}{m_{M^{2+}}} \Bigg/ \left(\frac{m_{H^{2+}}}{m_{M^{2+}}} + \frac{\sum \bar{q}_{M^{2+}}}{m_{M^{2+}}} \right) = \frac{\bar{m}_{M^{2+}}}{m_{M^{2+}}} \Bigg/ \left(1 + \frac{\sum \bar{q}_{M^{2+}}}{m_{M^{2+}}} \right) \quad (9)$$

A more convenient expression of eq 9 is obtained by identifying the measured and graphically determined distribution terms with the symbols, K_D^* and K_D, as shown in eq 9a. Rearrangement

$$K_D^* = K_D/(1 + \sum \bar{q}_{M^{2+}}/m_{M^{2+}}) \quad (9a)$$

of eq 9a leads to the following expression for $\sum \bar{q}_{M^{2+}}/m_{M^{2+}}$:

$$(K_D - K_D^*)/K_D^* = \sum \bar{q}_{M^{2+}}/m_{M^{2+}} \quad (10)$$

Division of both sides of equation 10 by Wm_{HPSS}, where W is the grams of water in the solvent sheath that is associated with 1 mmol of the polyelectrolyte solution, finally provides the sought for expression for $\bar{m}_{M^{2+}}/m_{M^{2+}}$:

$$\frac{K_D - K_D^*}{K^*_D W m_{HPSS}} = \frac{\sum \bar{q}_{M^{2+}}}{m_{M^2} W m_{HPSS}} = \frac{\bar{m}_{M^{2+}}}{m_{M^{2+}}} \quad (11)$$

For an estimate of $m_{H^+}/\bar{m}_{H^+}$ one need only divide $(\phi_{HPSS})(m_{HPSS})$ by $(1 - \phi_{HPSS})/Wm_{HPSS}$ as shown:

$$\frac{m_{H^+}}{\bar{m}_{H^+}} = \frac{\phi_{HPSS} W m_{HPSS}}{1 - \phi_{HPSS}} \quad (12)$$

By applying Gibbs–Donnan-based logic, once again, to describe counterion distribution patterns in the two separate regions that are presumed to constitute the polyelectrolyte solution at equilibrium, we find that

$$\ln \frac{(\bar{a}_{M^{2+}})}{(a_{M^{2+}})} \frac{(a_{H^+})^2}{(\bar{a}_{H^+})^2} = \ln \frac{K_D - K_D^*}{K_D^*} \frac{(\phi_{HPSS})^2 W m_{HPSS}}{(1 - \phi_{HPSS})^2} + \ln \frac{(\bar{\gamma}_{M^{2+}})}{(\gamma_{M^{2+}})} \frac{(\gamma_{H^+})^2}{(\bar{\gamma}_{H^+})^2} = 0 \quad (6c)$$

Because π, the pressure differential between the two regions of the polyelectrolyte is negligibly small, the $\pi(V_M - 2V_H)/RT$ term can be neglected as it has been in our presentation of eq 6c.

Values of W, the essential feature of our hypothetical model for solutions of linear, fully ionized polyelectrolytes become accessible with eq 6c. Because the values of $\bar{\gamma}_{H^+}$ and $\bar{\gamma}_{M^{2+}}$ are controlled by this quantity, the assessment of W with eq 6c cannot be straightforward, however. One must select a first value of W to provide a first estimate of the ionic strength of the counter-ion-concentrating domain of the polyelectrolyte with

$$\bar{I} = (1 - \phi_{HPSS})/W \quad (13)$$

The values of $\bar{\gamma}_{M^{2+}}$ and $\bar{\gamma}_{H^+}$ are then calculated with

$$\bar{\gamma}_{H^+} = \frac{(\gamma^{\pm}_{HCl})^2}{(\gamma^{\pm}_{KCl})} \quad (\bar{I} = I_{calc}) \quad (14)$$

$$\bar{\gamma}_{M^{2+}} = (\gamma^{\pm}_{MCl_2})^3/(\gamma^{\pm}_{KCl})^2 \quad (\bar{I} = I_{calc}) \quad (15)$$

using the mean molal activity coefficient values available in the literature for HCl, KCl, and MCl_2 at that ionic strength.[22]

The extra thermodynamic assumption that $\gamma_{K^+} = \gamma_{Cl^-}$ implied by this approach, is compatible with the fact that their transport numbers in solution are identical or nearly so over an extended concentration range.[26] Since they apparently have the same size in solution, their charge densities and as a consequence their activity coefficients are expected to be nearly identical as well. In addition, the estimate that $\bar{\gamma}_{H^+}$ and $\bar{\gamma}_{M^{2+}}$ at I_{calc} is the same as it is in solution at the same I value is believed to be a reasonable extra-thermodynamic assumption.

The value of W is then reassessed with eq 6c using the computed $\bar{\gamma}_{H^+}$ and $\bar{\gamma}_{M^{2+}}$ values. The procedure is repeated until the selected

TABLE II: Projection of log K_D Values with Eqs 16 and 17

m_{H^+}	log K_d exptl	log K_d eq 16[a]	log $K_{D(exp)}/K_D$(eq 16)	log K_D(eq 17)	log $K_{D(exp)}/K_D$(eq 17)
4.52	4.375	4.339	−0.036	4.365	−0.010
4.52	4.358	4.348	−0.010	4.374	+0.016
4.54	3.878	3.923	−0.045	3.928	+0.050
4.54	3.967	3.980	+0.013	3.988	+0.021
4.58	3.456	3.467	+0.011	3.448	−0.008
4.58	3.479	3.485	+0.006	3.467	−0.012
4.62	3.128	3.097	−0.031	3.059	−0.069

[a] Regression output for eq 16 (equation 17): constant 1.898 (1.800); standard error in constant 0.0306; slope −0.9422 (−0.990); standard error in slope 0.0249; r^2 0.9965; number of observations 7; degrees of freedom 5.

(23) Whitfield, M. In *Chemical Oceanography*; Riley, J. P., Skirrow, G., Eds.; Academic Press: London, 1975; Vol. 1, 106.
(24) Kielland, J. *J. Am. Chem. Soc.* **1937**, *59*, 1675.
(25) Reddy, M. M.; Marinsky, J. A. *J. Phys. Chem.* **1970**, *74*, 3884.
(26) Moore, W. J. *Physical Chemistry*, 4th ed.; Longmans: London, 1962; p 337.

TABLE III: Estimates of Trace Metal Ion Ratios (log K_D) for the Characterized Dowex 50 Resin and Different Polyelectrolyte Solutions (HPSS) at Equilibrium

m_{HPSS}	$\bar{m}_{H^+}$	K_D*	ϕ_{HPSS}	m_{H^+}	γ_{H^+}	$\gamma_{Co^{2+}}$	$\log (a_{H^+})^2/\gamma_{Co^{2+}}$	log K_D
0.973×10^{-3}	4.42	27060	0.22	2.14×10^{-4}	0.98	0.977	−7.344	9.07
0.978×10^{-3}	4.42	26567	0.22	2.15×10^{-4}	0.98	0.972	−7.340	9.07
2.41×10^{-2}	4.425	3277	0.22	5.30×10^{-3}	0.939	0.74	−4.475	6.23
2.42×10^{-2}	4.425	2991	0.22	5.32×10^{-3}	0.932	0.74	−4.475	6.23
4.61×10^{-2}	4.44	1494	0.225	1.02×10^{-2}	0.915	0.674	−3.889	5.65
5.82×10^{-2}	4.45	1098	0.23	1.34×10^{-2}	0.905	0.65	−3.647	5.41
1.06×10^{-1}	4.47	642	0.245	2.60×10^{-2}	0.879	0.575	−3.042	4.81
0.91×10^{-1}	4.46	649	0.24	2.18×10^{-2}	0.882	0.597	−3.208	4.98
1.628×10^{-1}	4.49	317	0.28	4.56×10^{-2}	0.861	0.494	−2.506	4.28
1.666×10^{-1}	4.49	299	0.28	4.66×10^{-2}	0.860	0.490	−2.484	4.26

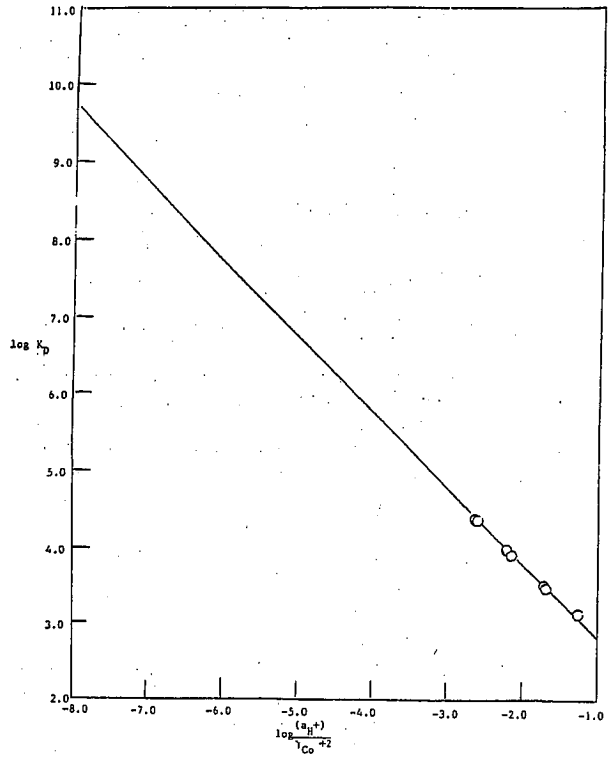

Figure 1. Plot of log K_D versus log $[(a_{H^+}{}^2)/\gamma_{Co^{2+}}]$ using resin characterization data summarized in Table I.

value of W agrees with the value computed using the W-based estimates of $\bar{\gamma}_{H^+}$ and $\bar{\gamma}_{M^{2+}}$.

IV. Experimental Section

The data employed to facilitate the research objectives that we have outlined were compiled in earlier research programs.[17,21,25] Detailed descriptions of the chemicals, their preparation, the apparatus, and the methods used are contained in these earlier publications.[17,21,25]

V. Results

A. Resin Calibration. Results from the sequence of operations that were carried out for the eventual evaluation of W as a function of polyelectrolyte concentration are presented in this section. To initiate this portion of the presentation, the ion-exchange data compiled for the characterization of the 8% divinylbenzene cross-linked poly(styrenesulfonic acid) resin (Dowex-50) are presented first in Table I. The molality of H^+ ion in the resin and solution phases of a particular experiment are listed in the first and second columns of this table. The distribution of ^{60}Co between resin and solution, measured at the various $HClO_4$ molalities (K_D), is presented next in column 3. The mean molal activity coefficient quotient of eq 6b, obtained by using literature-based values at the experimental $HClO_4$ concentration values,[22] expressed as shown in eq 6a, are given in column 4. The

TABLE IV: Comparison of Graphically Interpolated log K_D Values with Their Model-Based Estimates

	log K_D			log K_D	
m_{HPSS}	eq 17	eq 6c	m_{HPSS}	eq 17	eq 6c
0.973×10^{-3}	9.07	9.095	5.82×10^{-2}	5.41	5.403
0.978×10^{-3}	9.07	9.091	1.06×10^{-1}	4.81	4.803
2.41×10^{-2}	6.23	6.228	0.91×10^{-1}	4.98	4.970
2.42×10^{-2}	6.23	6.231	1.628×10^{-1}	4.29	4.271
4.61×10^{-2}	5.64	5.644	1.666×10^{-1}	4.26	4.250

logarithm of $a_{H^+}{}^2/\gamma_{Co^{2+}}$, obtained through multiplying the quantity listed in column 4 by the molality of $HClO_4$ squared, is presented in column 5. The quantity $\ln (\bar{\gamma}_{H^+})^2/(\bar{\gamma}_{Co^{2+}}) + \pi(2V_H - V_{Co})/RT$, resolved with eq 6a, is presented in the last column of the table. The probable error of 5.5% in this parameter approaches the variance that could be introduced, as discussed earlier, by neglecting the effect of electrolyte interaction on the activity coefficient of $Co(ClO_4)_2$, and suggests that neglect of this correction has not been a source of significant error in the resin characterization estimates.

To relate these K_D values to those associated with the equilibrium distribution of trace ^{60}Co between the 8% cross-linked gel and that portion of the polyelectrolyte solution that contains the fraction of H^+ ion that escapes from the solvated sheath of the polyelectrolyte molecule, an equation that best describes the Gibbs–Donnan-based projection of the straight line relationship that is expected between log K_D and log $(\alpha_{H^+})^2/\gamma_{Co^{2+}}$ in the resin characterization experiments was sought. Equation 16 provides

$$\log K_D = (1.898 \pm 0.0306) - (0.9422 \pm 0.0249) \log [(a_{H^+})^2/\gamma_{Co^{2+}}] \quad (16)$$

$$\log K_D = 1.800 - 0.990 \log (a_{H^+})^2/\gamma_{Co^{2+}} \quad (17)$$

the best fit to the experimental data. However, eq 17 has been selected for the K_D projections being sought because the projected slope of the line is much closer to the model-based value of −1.00 with minimal loss of predictive quality. That this is indeed the case may be seen from inspection of Table II, where the experimental log K_D values of the resin characterization program are compared with the log K_D values calculated using eqs 16 and 17.

The decision to use eq 17 instead of eq 16 is justified by the fact that the log K_D value measured in 0.168 m $HClO_4$ is the one most likely to deviate from the behavior predicted on the basis of resin invariance. It is this log K_D value that influences resolution of the smaller than predicted slope in the regression based eq 16.

The log K_D values obtained with eq 17, relating the equilibrium distribution of trace $^{60}Co^{2+}$ and H^+ ions between the resin and the various poly(styrenesulfonic acid) solutions, provide the variation of log K_D with log $[(a_{H^+})^2/\gamma_{Co^{2+}}]$ (Figure 1). These log K_D values are presented in the last column of Table III. The log $[(a_{H^+})^2/(\gamma_{Co^{2+}})]$ estimates based on such representation of the polyelectrolyte in solution are placed next to them in column 8 of Table III. Column 1 of Table III lists the molality, on a monomer basis, of the linear HPSS used in each equilibration. The H^+ ion molality of the gel phase in each experiment is given in column 2; K_D*, the measured distribution of trace $^{60}Co^{2+}$ ion

TABLE V: Water Uptake (grams) by the Counterion-Concentrating Region of 1 mmol (Monomer Basis) of Poly(styrenesulfonic acid)

m_{HPSS}	K_D	K_D^*	ϕ_{HPSS}	$\sum\bar{q}_{H^+}$	$\bar{\gamma}_{H^+}$	$\bar{\gamma}_{Co^{2+}}$	W
9.73×10^{-4}	1.24×10^{9}	2.706×10^{4}	0.22	7.589×10^{-4}	0.980	0.270	1.023
9.78×10^{-4}	1.23×10^{9}	2.654×10^{4}	0.22	7.628×10^{-4}	0.982	0.2695	1.005
2.41×10^{-2}	1.69×10^{6}	3.277×10^{3}	0.22	1.880×10^{-2}	0.850	0.2975	2.062
2.41×10^{-2}	1.70×10^{6}	2.991×10^{3}	0.22	1.888×10^{-2}	0.856	0.2957	1.930
4.61×10^{-2}	4.41×10^{5}	1.494×10^{3}	0.225	3.573×10^{-2}	0.865	0.293	1.800
5.82×10^{-2}	2.52×10^{5}	1.098×10^{3}	0.23	4.481×10^{-2}	0.869	0.291	1.718
1.06×10^{-1}	6.35×10^{4}	6.42×10^{2}	0.245	8.003×10^{-2}	0.863	0.293	1.745
9.10×10^{-2}	9.33×10^{4}	6.49×10^{2}	0.24	6.916×10^{-2}	0.877	0.288	1.582
1.628×10^{-1}	1.866×10^{4}	3.17×10^{2}	0.28	1.172×10^{-1}	0.893	0.281	1.339
1.666×10^{-1}	1.778×10^{4}	2.99×10^{2}	0.28	1.200×10^{-1}	0.899	0.278	1.308

between resin and HPSS, is listed in column 3 of the table. The osmotic coefficients presented in the next column are based on earlier vapor pressure osmometry measurements[17,21] and are used to provide column 5, which lists the molality of H^+ ion, $(\phi_{HPSS})(m_{HPSS})$, that is accessible to the K_D measurements. The single ion activity coefficients that are listed in columns 6 and 7 of Table III were obtained through use of Kielland's single ion activity coefficient tables.[24]

To examine the internal consistency of this approach, we have compared the above estimates of log K_D with those obtained by using eq 6b. This reevaluation of log K_D was accomplished by combining the averaged value of 0.461 that was obtained for the log $[(\bar{\gamma}_{H^+})^2/(\bar{\gamma}_{Co^{2+}})] + (\pi/2.3RT)(2V_{H^+} - V_{Co^{2+}})$ terms in the resin characterization study summarized in Table I with estimates of γ_{H^+} and $\gamma_{Co^{2+}}$ and the experimentally based values of $\bar{m}_{H^+}$, m_{HPSS}, and ϕ_{HPSS} in eq 6b.

$$\log K_D = \log \frac{(\bar{m}_{H^+})^2}{(m_{HPSS}\phi_{HPSS})^2} \frac{(\gamma_{Co^{2+}})}{(\gamma_{H^+})^2} + \log \frac{(\bar{\gamma}_{H^+})^2}{(\bar{\gamma}_{Co^{2+}})} + \pi \frac{[2V_{H^+} - V_{Co^{2+}}]}{2.3RT} \quad (6b)$$

The two sets of log K_D values are compared in Table IV and the excellent agreement between them provides the clear demonstration of internal consistency being sought.

B. Water Content of the Counterion-Concentrating Domain of HPSS, the Linear Polyelectrolyte Analogue of Dowex-50. Equation 6c developed earlier for the evaluation of W by equating the ratio of the electrochemical potential of the pairs of ions in the two separate regions of the linear polyelectrolyte solution at equilibrium with the resin phase and with each other has been used to compile the estimates of the W parameter that are presented in Table V. The items listed in the first four columns of this table appear earlier and have already been described. Column 5 presents for the first time the quantity of H^+ ion, in millimoles, that is presumed to be transferred to the solvent sheath of the polyion from a 1.0-g portion of the water that the polyelectrolyte is dissolved in $(\sum\bar{q}_{H^+} = (1 - \phi_{HPSS})(m_{HPSS}))$. The activity coefficient calculated for the H^+ and Co^{2+} ions contained by the counterion-concentrating sheath of the polyion are presented for the first time as well in columns 6 and 7 of Table V. The values of W, the solvent content of the polyion domain, are finally reported in column 8 as grams of water per millimole of HPSS. The iterative procedure used to resolve the W parameter for each of the systems studied is described in the sample calculation presented in the Appendix.

The internal consistency of this approach is demonstrable as well. One need only show that use of the W and $(\bar{\gamma}_{H^+})/(\bar{\gamma}_{Co^{2+}})$ values resolved in the iterative program leads to log K_{th} values equal to or very close to zero when the distribution of counterions in the resin and the counterion-concentrating domain of the polyion are examined with

$$\log K_D K_D^*/(K_D - K_D^*) \frac{(1 - \phi_{HPSS})^2 (m_{HPSS})(\bar{\gamma}_{H^+})^2}{(\bar{m}_{H^+})^2 (W)(\bar{\gamma}_{Co^{2+}})} + \log \frac{\bar{\gamma}_{Co^{2+}}}{(\bar{\gamma}_{H^+})^2} + \pi(V_{Co^{2+}} - 2V_{H^+}) = \log K_{th} = 0 \quad (6d)$$

To obtain eq 6d for this purpose $K_D K_D^* W(m_{HPSS})/(K_D - K_D^*)$ and $(1 - \phi_{HPSS})^2(m_{HPSS})^2/(\bar{m}_{H^+})^2(W)^2(m_{HPSS})^2$ are substituted for $\bar{m}_{Co^{2+}}/\bar{m}_{Co^{2+}}$ and $(\bar{m}_{H^+})^2/(\bar{m}_{H^+})^2$, which replace $\bar{m}_{Co^{2+}}/m_{Co^{2+}}$ and $(m_{H^+})^2/(\bar{m}_{H^+})^2$ in eq 6b and $\bar{m}_{Co^{2+}}/m_{Co^{2+}}$ and $(\bar{m}_{H^+})^2/(\bar{m}_{H^+})^2$ in eq 6c. Employment of W, $\bar{\gamma}_{H^+}$, and $\bar{\gamma}_{Co^{2+}}$ from the iterative program together with the value of −0.461 resolved for $[\log \bar{\gamma}_{Co^{2+}}/(\bar{\gamma}_{H^+})^2 + \pi((V_{Co^{2+}} - 2V_{H^+})/2.3RT)]$ in the resin calibration studies leads to the log K_{th} values presented in Table VI. They are very close to zero in value to provide further corroboration of the self-consistency of the approach.

TABLE VI: Evaluation of log K_{th} with Eq 6d

m_{HPSS}	log K_{th}	m_{HPSS}	log K_{th}
9.73×10^{-4}	−0.006	5.82×10^{-2}	0.002
9.78×10^{-4}	−0.001	1.06×10^{-1}	−0.005
2.41×10^{-2}	0.000	9.10×10^{-2}	0.004
2.42×10^{-2}	0.000	1.628×10^{-1}	−0.004
4.61×10^{-2}	0.014	1.666×10^{-1}	0.001

VI. Discussion

The success of the circuitous examinations of the Gibbs–Donnan-based apportionment of counterions to a solvent sheath of the polyion and the remainder of the solution external to it in the preceeding series of exercises cannot be claimed to have documented further the validity of this approach. However, the fact that such apportionment is consistent with the salt-sensitive properties of linear, weak-acid polyelectrolytes,[10,11] the ion-exchange behavior of fully dissociated linear polyelectrolytes,[17,21] and the mathematically deduced ion-condensation properties of linear polyelectrolytes[13,16] is believed to provide persuasive support for the model.

Because the reduced viscosity of polyelectrolytes is expected to be proportional to their shear volume in solution, there should be some correlation between reduced viscosity and the solvent content of the counterion-concentrating domain of a polyelectrolyte to provide additional support of the model. We have, as a consequence compared the reduced viscosity measurements, η_{sp}/c, reported in the literature for sodium poly(styrenesulfonate)[27] with our estimates of W for poly(styrenesulfonic acid) over the same molality (monomer basis) range in Figure 2 to bolster further Gibbs–Donnan based projections of the model. Except for the most dilute region examined, the trends of both reduced viscosity and W with molality are very similar. Both the reduced viscosity of polyelectrolyte solutions and the bulk of the polyelectrolytes increase with decreasing molality; the increase with decreasing molality of solvent uptake that is predicted by our model for the solvation sheath of the charged polyelectrolyte molecule is, in fact, in agreement with expectations based on the reduced viscosity pattern.

The sudden drop in the value of W at the lowest molality examined with the Gibbs–Donnan-based approach is anomalous. It must be noted, however, that the ϕ_{HPSS} estimate at this lowest concentration level had to be based on a linear extrapolation of the data. Any error in its reported value would be reflected in the extrapolated value of K_D, which would in turn affect the value of W that is eventually resolved.

A review of the literature does indeed indicate that the underestimate of W may, in part, be due to overestimate of ϕ_{HPSS}. This assessment was based on extrapolation of a plot of osmotic

(27) Prini, R. F.; Lagos, A. E. *Polym. Sci.* **1964**, *A2*, 2917.

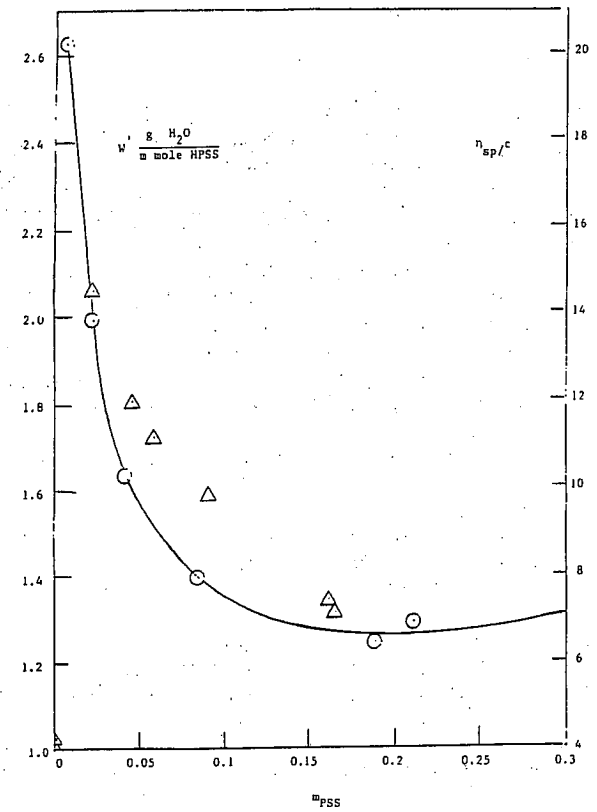

Figure 2. Comparison of reduced viscosity and solvent uptake patterns in polyelectrolytes as a function of molality (monomer basis): reduced viscosity, η_{sp}/c, of sodium polystyrene sulfonate;[27] Donnan-based estimates of water uptake (W) by counterion-concentrating domain of poly(styrenesulfonic acid).

coefficient versus polyelectrolyte molality (monomer basis) data that has been reported for a salt-free sodium poly(styrenesulfonate).[17,25] Linear extrapolation of these data to parallel the earlier treatment of the ϕ_{HPSS} data leads to a single ion activity coefficient of 0.21 at 9.7×10^{-4} m instead of the 0.11 value actually measured.[28] Such an error in our estimate of ϕ_{HPSS} at this molality would lead to a 40% underestimate of W. However, the corrected value of 1.4 g of H_2O/mmol of HPSS still leaves an abrupt discontinuity in the plot of W versus HPSS molality on passing from a 2.4×10^{-2} m solution to one that is 9.7×10^{-4} m.

The possibility that the source of such divergence from expected behavior, after correction for error in the estimate of ϕ_{HPSS}, can be attributed to experimental bias in the measurement of K_D^* is unlikely. For example, the unsuspected presence in the polyelectrolyte solution of simple electrolyte at a concentration level of at least 10^{-4} m would have been needed for significant disruption of the W computation.

Even though we are unable to explain the unexpectedly abrupt decrease in W that the Gibbs–Donnan-based approach projects for very dilute poly(styrenesulfonic acid) solutions the insight provided with respect to the properties of polyelectrolyte solutions is believed to merit its further use and development. For example, our earlier examination of the influence of simple salt concentration levels on the apparent binding of divalent ions to poly(styrenesulfonate) and dextran sulfate with this approach proved successful.[29] Visualization of a counterion-concentrating solvent sheath next to the charged surface of these polyelectrolytes permitted a quantitative interpretation of the observed sensitivity of divalent ion removal from solution to the counterion-concentration level of that particular solution of polyelectrolyte and simple salt.

(28) Oosawa, F. *Polyelectrolytes*; Marcel Dekker: New York, 1971; p 89, bottom curve of Figure 29b.
(29) Marinsky, J. A.; Baldwin, R.; Reddy, M. M. *J. Phys. Chem.* **1985**, *89*, 5.

Appendix

Presented is a sample calculation of W, the grams of water taken up by the counterion-concentrating domain of 1 mmol of poly(styrenesulfonic acid) (monomer basis).

System: Dowex-50 (8% DVB) resin in H^+ ion form, poly(styrenesulfonic acid), ^{60}Co.

System Parameters: $\bar{m}_H = 4.425$; $m_{HPSS} = 0.0241$; $\phi_{HPSS} = 0.22$; $K_D^* = 3.277 \times 10^3$; K_D (interpolated, Figure 1) $= 1.73 \times 10^6$:

$$\log \frac{\bar{\gamma}_{Co^{2+}}}{(\bar{\gamma}_{H^+})^2} + \frac{\pi(V_{Co} - 2V_H)}{2.3RT} = -0.461$$

Step 1: Employment of eq 6d for evaluation of $W(\bar{\gamma}_{Co^{2+}})/(\bar{\gamma}_{H^+})^2$:

$$\log \frac{K_D K_D^*}{K_D - K_D^*} \frac{(1 - \phi_{HPSS})^2 (m_{HPSS})}{(\bar{m}_{H^+})^2} + \log \frac{\bar{\gamma}_{Co^{2+}}}{(\bar{\gamma}_{H^+})^2} + \pi \frac{(V_{Co} - 2V_H)}{2.3RT} = \log W \frac{(\bar{\gamma}_{Co^{2+}})}{(\bar{\gamma}_{H^+})^2}$$

$$-0.071 = \log W \frac{(\bar{\gamma}_{Co})}{(\bar{\gamma}_{H^+})^2}$$

$$0.849 = W \frac{(\bar{\gamma}_{Co})}{(\bar{\gamma}_{H^+})^2} = \left(\frac{\text{g of } H_2O}{\text{mmol of HPSS}} \right) \bar{\gamma}_{Co^{2+}} / (\bar{\gamma}_{H^+})^2$$

Step 2: Evaluation of W: Let

$$W = \frac{2.0 \text{ g of } H_2O}{\text{mmol of HPSS}}$$

then

$$\bar{I} = \frac{1 - \phi_{HPSS}}{W'} = \frac{0.78}{2.00} = 0.39$$

and

$$\bar{\gamma}_{H^+} = \frac{(\gamma^{\pm}_{HCl})^2}{(\gamma^{\pm}_{KCl})}$$

at $\bar{I} = 0.39$

$$\bar{\gamma}_{H^+} = \frac{(0.755)^2}{0.6682} = 0.853$$

$$\bar{\gamma}_{Co^{2+}} = (\gamma^{\pm}_{CoCl_2})^3 / (\gamma^{\pm}_{KCl})^2$$

at $\bar{I} = 0.39$

$$\bar{\gamma}_{H^+} = \frac{(0.5098)^3}{(0.6682)^2} = 0.297$$

and

$$W = 0.849(\bar{\gamma}_{H^+})^2/(\bar{\gamma}_{Co}) = 8.49(0.853)^2/297 = 2.08 \text{ g of } H_2O/\text{mmol of HPSS}$$

Now let

$$W = 2.062 \text{ g of } H_2O/\text{mmol of HPSS}$$

then

$$\bar{I} = 0.78/2.062 = 0.3783$$

and

$$\bar{\gamma}_{H^+} = \frac{(\gamma^{\pm}_{HCl})^2}{(\gamma^{\pm}_{KCl})}$$

at $\bar{I} = 0.3783$

$$\bar{\gamma}_{H^+} = \frac{(0.755)^2}{(0.6726)} = 0.8475$$

$$\bar{\gamma}_{Co^{2+}} = \frac{(\gamma^{\pm}_{CoCl_2})^3}{(\gamma^{\pm}_{KCl})^2}$$

at $\bar{I} = 0.3783$

$$\bar{\gamma}_{H^+} = \frac{(5115)^3}{(0.6726)^2} = 0.296$$

and

$W = 0.849(0.8475)^2/0.296 =$

2.060 g of H_2O/mmol of HPSS

W selected $= \frac{2.062 \text{ g of } H_2O}{\text{mmol of HPSS}}$; W value returned =

2.060 QED